# Calculational and Experimental Investigations of the Pressure Effects on Radical−Radical Cross Combination Reactions: $C_2H_5 + C_2H_3$†

**Askar Fahr,*,‡ Joshua B. Halpern,‡ and Dwight C. Tardy*,§**

*Department of Chemistry, Howard University, Washington, D.C. 20059, Department of Chemistry, The University of Iowa, Iowa City, Iowa 52242*

*Received: November 7, 2006; In Final Form: May 17, 2007*

Pressure-dependent product yields have been experimentally determined for the cross-radical reaction $C_2H_5 + C_2H_3$. These results have been extended by calculations. It is shown that the chemically activated combination adduct, 1-$C_4H_8$*, is either stabilized by bimolecular collisions or subject to a variety of unimolecular reactions including cyclizations and decompositions. Therefore the "apparent" combination/disproportionation ratio exhibits a complex pressure dependence. The experimental studies were performed at 298 K and at selected pressures between about 4 Torr (0.5 kPa) and 760 Torr (101 kPa). Ethyl and vinyl radicals were simultaneously produced by 193 nm excimer laser photolysis of $C_2H_5COC_2H_3$ or photolysis of $C_2H_3Br$ and $C_2H_5COC_2H_5$. Gas chromatograph/mass spectrometry/flame ionization detection (GC/MS/FID) were used to identify and quantify the final reaction products. The major combination reactions at pressures between 500 (66.5 kPa) and 760 Torr are (1c) $C_2H_5 + C_2H_3 \rightarrow$ 1-butene, (2c) $C_2H_5 + C_2H_5 \rightarrow$ *n*-butane, and (3c) $C_2H_3 + C_2H_3 \rightarrow$ 1,3-butadiene. The major products of the disproportionation reactions are ethane, ethylene, and acetylene. At moderate and lower pressures, secondary products, including propene, propane, isobutene, 2-butene (cis and trans), 1-pentene, 1,4-pentadiene, and 1,5-hexadiene are also observed. Two isomers of $C_4H_6$, cyclobutene and/or 1,2-butadiene, were also among the likely products. The pressure-dependent yield of the cross-combination product, 1-butene, was compared to the yield of *n*-butane, the combination product of reaction (2c), which was found to be independent of pressure over the range of this study. The [1-$C_4H_8$]/[$C_4H_{10}$] ratio was reduced from ∼1.2 at 760 Torr (101 kPa) to ∼0.5 at 100 Torr (13.3 kPa) and ∼0.1 at pressures lower than about 5 Torr (∼0.7 kPa). Electronic structure and RRKM calculations were used to simulate both unimolecular and bimolecular processes. The relative importance of C−C and C−H bond ruptures, cyclization, decyclization, and complex decompositions are discussed in terms of energetics and structural properties. The pressure dependence of the product yields were computed and dominant reaction paths in this chemically activated system were determined. Both modeling and experiment suggest that the observed pressure dependence of [1-$C_4H_8$]/[$C_4H_{10}$] is due to decomposition of the chemically activated combination adduct 1-$C_4H_8$* in which the weaker allylic C−C bond is broken: $H_2C{=}CHCH_2CH_3 \rightarrow C_3H_5 + CH_3$. This reaction occurs even at moderate pressures of ∼200 Torr (26 kPa) and becomes more significant at lower pressures. The additional products detected at lower pressures are formed from secondary radical−radical reactions involving allyl, methyl, ethyl, and vinyl radicals. The modeling studies have extended the predictions of product distributions to different temperatures (200−700 K) and a wider range of pressures ($10^{-3}$−$10^5$ Torr). These calculations indicate that the high-pressure [1-$C_4H_8$]/[$C_4H_{10}$] yield ratio is 1.3 ± 0.1.

## Introduction

Free radicals are among the critical intermediates in hydrocarbon reaction systems. Small unsaturated hydrocarbon radicals are particularly important. Relatively little is known about the kinetics and dynamics of radical−radical reactions involving unsaturated radicals. Hydrocarbon radical termination reaction rates and their product yields are of great importance for understanding and modeling combustion[1−3] and atmospheric reaction systems.[4] Vinyl radical reactions are believed to be particularly important in high-temperature hydrocarbon combustion as well as in low-temperature planetary atmospheres.[1−4]

A number of papers from our laboratortory have previously reported on the kinetics and products of vinyl radical reactions[5−7] as well as the cross-radical reaction $C_2H_5 + C_2H_3 \rightarrow$ products (1) at ambient temperature and pressures up to 700 Torr (93 kPa).[8] Major products of reaction (1) at room temperature were identified by GC/MS/FID analysis. These include 1-butene, *n*-butane, and 1,3-butadiene formed, respectively, through the combination reactions: (1c) $C_2H_5 + C_2H_3 \rightarrow$ 1-butene, (2c) $C_2H_5 + C_2H_5 \rightarrow$ *n*-butane, and (3c) $C_2H_3 + C_2H_3 \rightarrow$ 1,3-butadiene. An overall rate constant of $k_1 = (9.6 \pm 1.9) \times 10^{-11}$ cm$^3$ molecule$^{-1}$ s$^{-1}$ was directly measured using time-resolved UV absorption spectroscopy. In addition, products of the disproportionation reaction, ethane, ethylene, and acetylene, were identified and quantified. From the product yields and relative rate measurements, a rate constant was derived for the cross-combination reaction $k_{1c} = (6.5 \pm 1)10^{-11}$ cm$^3$ molecule$^{-1}$ s$^{-1}$.

† Part of the special issue "M. C. Lin Festschrift".

* Corresponding authors. E-mail: afahr@msrce.howard.edu (A.F.); dwight-tardy@uiowa.edu (D.C.T.).

‡ Department of Chemistry, Howard University.

§ Department of Chemistry, The University of Iowa.

10.1021/jp067357v CCC: $37.00 
Published on Web 06/22/2007

Sequential reactions of chemically activated combination product are particularly important for any study of radical−radical reactions. Recent reports indicate a significant pressure effect on product distributions for the radical−radical reactions $CH_3 + C_2H_3$[5,9−11] and $C_2H_3 + C_2H_3$.[6,7] Separate studies demonstrate that the total radical−radical rate constants for these reactions are generally independent of pressure; however, product yields vary greatly in such reactions involving unsaturated radicals. For example, in the reaction $CH_3 + C_2H_3$, the contribution of the combination channel leading to propene declines from about 78% at pressures higher than ∼200 Torr (26.6 kPa) to about 39% at pressures of a few Torr. At low pressures, an additional reaction channel producing allyl radical ($C_3H_5$) and H-atoms becomes competitive with collisional stabilization.[5,9−11] Similarly, for the reaction $C_2H_3 + C_2H_3$ at pressures higher than roughly 10 Torr (1.3 kPa), the combination reaction producing 1,3-butadiene is the major channel, with a yield of about 70% and a combination/disproportionation ratio = [1,3-butadiene]/[ethylene] = 3.4 ± 0.3. The contribution of the product channel yielding 1,3-butadiene decreases with pressure; at about 3 Torr (0.36 kPa), the [1,3-butadiene]/[ethylene] ratio is ∼0.6.[6,7] At low pressures, various isomeric forms of the $C_4H_6$ combination product (1,2-butadiene and/or cyclobutene), as well as a number of $C_5$ and $C_6$ products not present significantly at high pressures, have been detected. In contrast to reactions involving unsaturated radicals, no pressure effect has been observed for the product channels of the $C_2H_5 + C_2H_5$ reaction over a pressure range of ∼2−700 Torr.[12] Product analysis for that reaction indicates that the ratio of combination/disproportionation = [*n*-$C_4H_{10}$]/[$C_2H_4$] remains constant within experimental error at 7.8 ± 0.7.

In general, combination reactions of unsaturated hydrocarbon radicals produce an excited combination product with large excess energy. The rates of these reactions are primarily determined by the formation of the combination product, not its ultimate fate. This suggests that the reverse reaction is relatively insignificant. However, as mentioned above for the reactions $CH_3 + C_2H_3$ and $C_2H_3 + C_2H_3$, yields of the product channels of radical−radical reactions can vary with changes in pressure. Results on the reaction $C_2H_3 + C_2H_3$ show that there is a competition between collisional deactivation and unimolecular reactions even at pressures of ∼1 atm, which accounts for the observed changes in relative product yields. Consequently, the pressure dependence of yields from unimolecular steps appears as a pressure dependence of the combination/disproportionation ratio.

This is the first reported study of pressure effects on the cross-reaction of ethyl and vinyl radicals. The open reaction pathways are compared to recently reported results for the cross combination of allyl and methyl radicals to form 1-butene. The work presented here extends our efforts, systematically combining experiment and calculation to understand complex pressure effects on the reaction kinetics and mechanisms of hydrocarbon radical−radical reactions. It is a truism that it is much easier to measure reaction rate constants than product yields, but the latter are as, if not more, important. Theoretically based calculation has become increasingly useful for elucidation of product yields. Even where product yields are known for a limited set of pressure and temperature conditions, calculation is necessary to extend the experimental results to important regimes. The set of experimentally determined product yields for a reaction can be both extremely difficult to measure and limited in range. In such cases, this being one, the only accessible pathway is to use theoretical calculations where the role of measurements is to provide a check on the theory.

## Procedures

**1. Experiment.** Experiments were performed using excimer laser photolysis: gas chromatograph/mass spectrometry/flame ionization detection (GC/MS/FID) end-product analysis. The experimental methods have been described elsewhere[8] and are expanded on in the Supporting Information, hence only a brief description will be given here. Ethyl and vinyl radicals were simultaneously produced in equal amounts from 193 nm photolysis of dilute mixtures of ethyl vinyl ketone ($C_2H_5$-$COC_2H_3$, EVK) in He. The photolysis samples contain a small amount of the radical precursor, usually in the range of about $1 \times 10^{15}$ to $6 \times 10^{16}$ molecule $cm^{-3}$, in an excess of He. Two self-enclosed gas circulating pumps, operational up to atmospheric pressure, were used to flow the gas mixture through the reaction cell so that the cell contents were replaced between as the photolysis laser was pulsed at a 0.5−2 Hz repetition rate. A total system volume of about 2000 times that of the active photolysis volume was used. Because of the removal of the photolyzed sample and significant dilution of products, secondary reactions due to product photolysis are not important. End-product analysis was performed using a specially modified, on-line Hewlett-Packard 6890 series gas chromatograph (GC) coupled to a 5970 series mass spectrometer (MS) and flame ionization detector (FID). The photolyzed sample was admitted to an evacuated injection loop that was immersed in liquid $N_2$. The content of the reaction manifold was passed through the loop and reaction products were collected, while the He inert gas was pumped out. The concentrated sample was warmed to room temperature and directly injected onto two separate $Al_2O_3$-coated capillary columns (HP-19095P) by admitting the carrier gas into the collection loop. Temperature programming of the GC oven was required to separate the products. However, it is possible that not all the isomeric forms of the products are separated under the flow and temperature conditions of the GC runs. The retention times and response of the FID and MS were calibrated by injection of available known standard samples with concentrations similar to those produced as a result of the laser photolysis and subsequent reactions.

The radical precursor was obtained commercially and was purified by trap-to-trap distillation. Ultrahigh purity He (99.9999%) was used for sample preparation and as the carrier gas for the gas chromatograph.

**2. Calculation.** *Enumeration of Potential Reactions.* The chemically activated 1-butene product results from the combination of ethyl and vinyl radicals. The competition between bimolecular collisional stabilization of the chemically activated adduct and unimolecular processes are expected to produce a pressure dependence. However, the competing disproportionation reactions that involve an intermolecular hydrogen migration from a donor to an acceptor is not expected to exhibit a pressure dependence because the energy released will be distributed between the two sets of products. Three classes of unimolecular reactions are available: simple C−H bond rupture, simple C−C bond rupture, and isomerization (cyclization/decyclization) involving H-atom migration. These reactions will be designated as C−H, C−C, and cycH, respectively. The decyclization (the reverse of the cyclization) reaction will be symbolized as -cycH. The combination (*c*), disproportionation (*d*), stabilization (*S*), and decomposition (*D*) steps used in the modeling of the $C_2H_5 + C_2H_3$ reaction are listed below. Vibrational excitation is designated by an * following the

**TABLE 1: Experimental Conditions and Yields of the Major Final Products ($10^{12}$, molecule $cm^{-3}$) Following the 193 nm Photolysis of Mixtures of EVK in He at $T = 298$ K and a Total Pressure of 700 Torr (93 kPa)**

| [EVK][a] | laser $E$[b] | [$C_2H_2$] | [$C_2H_4$] | [$C_2H_6$] | [1,3-$C_4H_6$] | [1-$C_4H_8$] | [$n$-$C_4H_{10}$] |
|---|---|---|---|---|---|---|---|
| $6.5 \times 10^{15}$ | ~200 mJ | 13.1 | 25.4 | 8.9 | 27.7 | 37.2 | 36.2 |
| $8.0 \times 10^{15}$ | ~130 | 8.2 | 20.8 | 7.8 | 21.4 | 28.0 | 27.5 |
| $6.5 \times 10^{15}$ | ~70 | 5.4 | 9.9 | 7.6 | 11.3 | 13.9 | 12.8 |
| $13 \times 10^{15}$ | ~75 | 12.1 | 18.7 | 8.2 | 22.9 | 33.6 | 29.8 |

[a] Molecule $cm^{-3}$. [b] Laser energy as monitored at the source.

chemical formula. For reactants, the number preceding a chemical formula indicates the position of unsaturation, while for products, the unsaturation position does not change. The number after the chemical formula designates the position of the "free" electron in the radical. For methyl cyclopropane ($CH_3$-$c$-$C_3H_5$), the methyl or ring C−H bonds can dissociate; these are designated by C−H or C−H′, respectively. Likewise if a ring C−H bond is involved in the decyclization, then this is designated as $k_{-\mathrm{cycH'}}$

Disproportionation:

| | | |
|---|---|---|
| $C_2H_5 + C_2H_3 \rightarrow C_2H_4 + C_2H_4$ | $k_{1d}$ | (1) |
| $C_2H_3 + C_2H_5 \rightarrow C_2H_2 + C_2H_6$ | $k_{1d'}$ | (2) |

Combination:

| | | |
|---|---|---|
| $C_2H_5 + C_2H_3 \rightarrow$ 1-$C_4H_8$* | $k_{1c}$ | (3) |

isomerization:

| | | |
|---|---|---|
| 1-$C_4H_8$* ⇆ $CH_3$-$c$-$C_3H_5$* | $k_{\mathrm{cycH}}$, $k_{-\mathrm{cycH'}}$ | (−4,4) |
| $CH_3$-$c$-$C_3H_5$* ⇆ *cis*-2-$C_4H_8$* | $k_{-\mathrm{cycH'}}$, $k_{\mathrm{cycH}}$ | (5,−5) |
| $CH_3$-$c$-$C_3H_5$* ⇆ *trans*-2-$C_4H_8$* | $k_{-\mathrm{cycH'}}$, $k_{\mathrm{cycH}}$ | (6,−6) |
| $CH_3$-$c$-$C_3H_5$* ⇆ *iso*-$C_4H_8$* | $k_{-\mathrm{cycH}}'$, $k_{\mathrm{cycH}}$ | (7,−7) |

decomposition:

| | | |
|---|---|---|
| 1-$C_4H_8$* → $C_2H_5 + C_2H_3$ | $k_{-1c} = k_{C-C}$ | (8) |
| 1-$C_4H_8$* → $C_3H_5 + CH_3$ | $k_{C-C}$ | (9) |
| 1-$C_4H_8$* → $C_4H_7$-(3) + H | $k_{C-H}$ | (10) |
| 1-$C_4H_8$* → $C_4H_7$-(1, 2, or 4) + H | $k_{C-H}$ | |
| *cis*-2-$C_4H_8$* → $C_3H_5$-(1) + $CH_3$ | $k_{C-C}$ | |
| *cis*-2-$C_4H_8$* → $C_4H_7$-(1) + H | $k_{C-H}$ | (11) |
| *cis*-2-$C_4H_8$* → $C_4H_7$-(2) + H | $k_{C-H}$ | |
| *trans*-2-$C_4H_8$* → $C_3H_5$-(1) + $CH_3$ | $k_{C-C}$ | |
| *trans*-2-$C_4H_8$* → $C_4H_7$-(1) + H | $k_{C-H}$ | (12) |
| *trans*-2-$C_4H_8$* → $C_4H_7$-(2) + H | $k_{C-H}$ | |
| *iso*-$C_4H_8$* → $C_3H_5 + CH_3$ | $k_{C'-C}$ | |
| *iso*-$C_4H_8$* → $C_4H_7$-(3 or 4) + H | $k_{C-H}$ | (13) |
| *iso*-$C_4H_8$* → $C_4H_7$-(1 or 2) + H | $k_{C-H}$ | |
| $CH_3$-$c$-$C_3H_5$* → $CH_2$-$c$-$C_3H_6$ + H | $k_{C-H}$ | |
| $CH_3$-$c$-$C_3H_5$* → $CH_3$-c-$C_3H_5$ (1 or 2) + H | $k_{C-H'}$ | |

stabilization:

| | | |
|---|---|---|
| 1-$C_4H_8$* + M → 1-$C_4H_8$ + M | $k_S$ | (14) |
| $CH_3$-$c$-$C_3H_5$* + M → $CH_3$-$c$-$C_3H_5$ + M | $k_S$ | (15) |
| *cis*-2-$C_4H_8$* + M → *cis*-2-$C_4H_8$ + M | $k_S$ | (16) |
| *trans*-2-$C_4H_8$* + M → *trans*-2-$C_4H_8$ | $k_S$ | (17) |
| *iso*-$C_4H_8$* + M → *iso*-$C_4H_8$ | $k_S$ | (18) |

The numbers given in parenthesis after the radical species indicate the position of the radical center. Reactions that are not numbered are unimportant for the present study.

## Results and Discussion

**1. Experimental.** The 193 nm photolysis of $C_2H_5COC_2H_3$ (EVK) generates ethyl and vinyl radicals with nearly identical yields.[8] Product studies were performed at 298 K and at selected pressures between ~3 Torr (0.4 kPa) and 760 Torr (~100 kPa). Final reaction products were identified and quantified using GC/MS/FID analysis. Examples of the mass spectra and FID traces from the final product analysis of EVK samples photolyzed at different pressure conditions and more information on the data analysis are available in the Supporting Information. The experimental study focused on the effect of pressure on the primary combination reactions (1c) and (2c) which produce, 1-butene and *n*-butane respectively. Experimental quantification of how pressure effects the yields of all the detectable final products, while feasible, would require calibration samples of each product including isomeric forms in order to quantitatively determine their GC retention times and the MS and FID detector response factors. The scope of such a study would be enormous.

**TABLE 2: Experimentally Determined Relative Yield of 1-Butene and *n*-Butane, [1-$C_4H_8$]/[$n$-$C_4H_{10}$] at $T = 298$ K and at Various Total Pressures**

| $P$ (Torr/kPa) | [1-$C_4H_8$]/[$n$-$C_4H_{10}$] |
|---|---|
| 760/101 | $1.20 \pm 0.10$[a] |
| 700/93 | 1.07 |
| 600/80 | 1.10 |
| 500/66 | $1.10 \pm 0.07$[a] |
| 100/13.3 | 0.40 |
| 80/10.5 | 0.78 |
| 63/8.4 | 0.41 |
| 11/1.5 | 0.30 |
| 4.1/0.55 | 0.20 |
| 3.5/0.46 | 0.07 |

[a] The listed uncertainties are determined from at least three measurements from separate experiments at nearly identical experimental conditions.

Major reaction products at pressures above ~500 Torr are 1-butene, *n*-butane, and 1,3-butadiene formed, respectively, through the combination reactions: $C_2H_5 + C_2H_3 \rightarrow$ 1-butene (1c), $C_2H_5 + C_2H_5 \rightarrow$ *n*-butane (2c), and $C_2H_3 + C_2H_3 \rightarrow$ 1,3-butadiene (3c). Ethane, ethylene, and acetylene resulting from disproportionation reactions were also observed as were a number of other minor products.

Table 1 describes the experimental conditions and the yield of the major final products at $T = 298$ K and 700 Torr (93 kPa) pressure as derived from calibrated GC/MS product analysis.

Minor quantities of 2-butene (cis and/or trans isomeric forms) or isobutene were found, with yields of about 5% relative to 1-butene. Several $C_3$, $C_5$, and $C_6$ hydrocarbon products were also identified at these pressures. At the highest total pressures, the following reactions should dominate.

| | |
|---|---|
| $C_2H_5COC_2H_3 + h\nu \rightarrow C_2H_5 + C_2H_3 + CO$ | |
| $C_2H_5 + C_2H_3 + M \rightarrow$ 1-$C_4H_8$ + M | $k_{1c}$ |
| $C_2H_3 + C_2H_5 \rightarrow C_2H_2 + C_2H_6$ | $k_{1d}$ |
| $C_2H_3 + C_2H_5 \rightarrow C_2H_4 + C_2H_4$ | $k_{1d'}$ |
| $C_2H_5 + C_2H_5 + M \rightarrow C_4H_{10}$ | $k_{2c}$ |
| $C_2H_5 + C_2H_5 \rightarrow C_2H_4 + C_2H_6$ | $k_{2d}$ |
| $C_2H_3 + C_2H_3 + M \rightarrow$ 1,3-$C_4H_6$ | $k_{3c}$ |
| $C_2H_3 + C_2H_3 \rightarrow C_2H_2 + C_2H_4$ | $k_{3d}$ |

The yield of 1-butene, at various pressures and at $T = 298$ K, was compared to the yield of *n*-butane formed from the self-combination of ethyl radicals. The combination reaction between ethyl radicals (2c), within the pressure range of this study, has been shown to be independent of pressure[8,12] Table 2 and Figure 1 display the experimental [1-$C_4H_8$]/[$C_4H_{10}$] values at various pressures.

At the highest pressures used in this study, an experimental value of [1-$C_4H_8$]/[$C_4H_{10}$] ~ 1.2 is obtained. Unfortunately, the

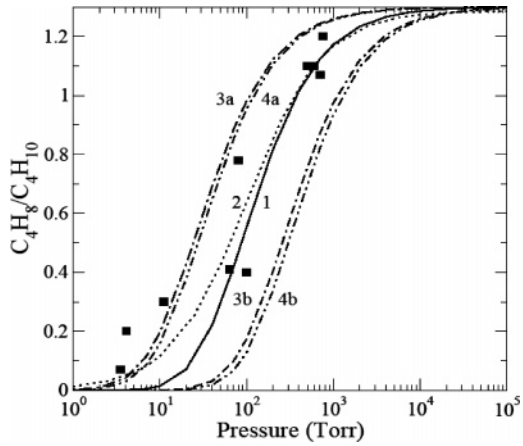


**Figure 1.** Calculated curves (1−4) and experimental points (filled squares) for the product ratio $[1\text{-}C_4H_8]/[C_4H_{10}]$ as a function of pressure at 298 K. The parameters used to generate curve 1 (solid line) are from B3LYP calculations for vibrational frequencies, the *A* factor ($1.02 \times 10^{16}$ $s^{-1}$) and $E_0$ (25100 $cm^{-1}$) for the bond dissociation energy. Curve 2 (dotted line) is a two-parameter (high-pressure limiting value and rate coefficient) least-squares fit to the experimental data. Curves 3a and 3b (dash−dash−dot lines) result when $E_0$ is increased and decreased by 1000 $cm^{-1}$ from the values used for curve 1. Curves 4a and 4b (dash−dot−dot lines) results when *A* is 0.3 and 3 times the value used in curve 1. Statistical errors limits on each point are ∼0.1

calculated high-pressure value of $[1\text{-}C_4H_8]/[C_4H_{10}]$ cannot be tested by the present experiments as pressures above 1 atm are not feasible with the apparatus used for this study Figure 1 indicates a high-pressure ratio of $[1\text{-}C_4H_8]/[C_4H_{10}] \sim 1.3$. This ratio decreases to about 0.5 at 100 (13 kPa) Torr and to less than about 0.1 at pressures below 4 Torr (∼0.6 kPa). The measurement uncertainties of the $[1\text{-}C_4H_8]/[C_4H_{10}]$ ratio, determined from repetitive experiments at higher pressures, were typically about 10%. However, at low pressures, the uncertainties tend to be larger.

The GC/MS/FID spectra from the end-product analysis of photolyzed EVK samples were congested, particularly at lower pressures, with peaks representing a large number of additional and isomeric products that were not present at a significant level, relative to butane, at higher pressures. The detected products included propene, propane, at least three isomers of $C_4H_8$, 1-pentene, 1,4-pentadiene, 1,5-hexadiene, and two isomeric forms of $C_4H_6$.

The presence of products such as pentadiene, 1-pentene, and 1,5-hexadiene, particularly at lower pressures, suggests the formation of allyl radicals. The subsequent self-reactions and cross-combination reactions of allyl radicals with ethyl and vinyl radicals would yield:

$$C_2H_5 + C_2H_3 \rightarrow 1\text{-}C_4H_8^* \rightarrow C_3H_5 + CH_3$$
$$C_3H_5 + C_2H_5 \rightarrow 1\text{-pentene}$$
$$C_3H_5 + C_2H_3 \rightarrow 1,4\text{-pentadiene}$$
$$C_3H_5 + C_3H_5 \rightarrow 1,5\text{-hexadiene}$$

In general, due to the higher density of internal eigenstates for comparable critical energies, the $C_5$ combination products will have a smaller unimolecular rate coefficient than the $C_4$ combination products. Hence, the collisional deactivation of the $C_5$ and $C_6$ products resulting from radical combination will dominate at all pressures used in the current study.

Isobutene and 2-butene isomers can be formed by sequential reversible isomerizations; first the isomerization of the chemically activated combination adduct $C_4H_8^*$ to methylcyclopropane (−4) followed by reversible decyclization of methylcyclopropane to either *cis*-2-butene (5) or *trans*-2-butene (6) or isobutene (7). These chemically activated $C_4$ isomers can subsequently either be collisionally stabilized (15, 16, 17, and 18), decompose via allylic C−H rupture (11, 12, and 13) or isomerize back to methylcyclopropane (−5, −6, −7).

In our ongoing study of pressure effect on product channels for the $C_2H_3 + C_2H_3$ system, we have observed the formation of cyclobutene, 1,2-butadiene, and 1,5-hexadiyne at very low pressures. Computational modeling suggested that cyclobutene and 1,2-butadiene can be formed from the isomerization of excited 1,3-butadiene, the combination product of vinyl radicals (3c). Propargyl and methyl radicals were also produced at low pressures by the sequential decomposition of 1,2-butadiene:

$$C_2H_3 + C_2H_3 \rightarrow C_4H_6^* \rightarrow 1,2\text{-butadiene}^* \rightarrow C_3H_3 + CH_3$$

Support for this scheme was based on the detection of $C_6H_6$ products. One of the $C_6H_6$ products matched both the retention time and the MS fragmentation pattern of 1,5-hexadiyne (the combination product of the self-combination of propargyl radicals). The second $C_6H_6$ peak could not be identified with certainty, but it did not match the retention time and MS fragmentation pattern of benzene.

The energetics and rate coefficients for unimolecular reactions leading to isomerization and decomposition are examined in the following section. The calculated results for the pressure dependence of product yields are then compared with the experimental observations of the 1-butene and *n*-butane ratio. Finally, the effect of temperature on the product distribution and the apparent rate coefficient is calculated.

**2. Computational Methodology.** *General Calculational Setup.* The chemical system presented in this paper can be represented by the following scheme abbreviated for strong collisions:

| | | |
|---|---|---|
| Formation: | $R + R' \rightarrow R_i(E)$ | $f(E)$ |
| Isomerization: | $R_i(E) \rightarrow R_j(E')$ | $k_{ji}(E)$ |
| Decomposition: | $R_i(E) \rightarrow D_{ia}$ | $k_{ia}(E)$ |
| Stabilization: | $R_i(E) + M \rightarrow S_i$ | $\omega$/[M] |

where *R* and *R′* are the ethyl and vinyl radicals, and $S_1-S_5$ are stabilized 1-butene, methylcyclopropane, *cis*-2-butene, *trans*-2-butene, and isobutene, respectively. $D_{1a}$, $D_{3a}$, $D_{4a}$, and $D_{5a}$ are the products from the allylic C−H bond ruptures in 1-butene, *cis*-2-butene, *trans*-2-butene, and isobutene, respectively, and $D_{1b}$ is the product from the allylic C−C bond rupture in 1-butene. The nascent 1-butene is formed with a thermal distribution of energies, $f(E)$, displaced by the energy released from the combination reaction. The rate coefficient for collisional stabilization is determined by the collision frequency, $\omega$, and the collider concentration, [M], i.e., the pressure. The $k_{ij}(E)$'s are the microscopic rate coefficients for the conversion between the *j*th and *i*th $C_4H_8$ isomers; $k_{ia}(E)$ is the microscopic rate coefficient from the *i*th isomer via channel a. Energy conservation relates reaction exo/endo ergicity to isoenergetic levels of isomers *i* and *j*: $\Delta E(j \rightarrow i) = E_0(j) - E_0(i)$. A set of coupled differential equations for each energy level of each isomer is solved and the yields of each product are then calculated as a function of time. For the present pulsed experiments only total (infinite time) yields of the products are measured. However, kinetic simulations indicate that steady-state calculations are sufficient to reproduce the pressure dependencies for the total 1-butene and butane yields reported here. Thus our calculated results are based on the time-independent (steady-state) solution of the coupled equations.

The strong collision scheme can be expanded to include weak collisions; the details and solution of this have been reported earlier.[15] Briefly, weak collisions "couple" the energy levels

**TABLE 3: Thermodynamic and Kinetics Parameters for the $C_4H_8$ System (Energies in $cm^{-1}$)**

| reaction | $\Delta E^a$ $cm^{-1}$ | $E_o{}^b$ $cm^{-1}$ | $E_a$(calc)$^c$ $cm^{-1}$ | $E_a$(lit)$^d$ $cm^{-1}$ | $A$ (calc)$^e$ 1/s | $A$(lit)$^d$ 1/s | $Q(P)/Q(R)^e$ |
|---|---|---|---|---|---|---|---|
| 1-butene → butenyl-3 + H | 29300 | 29300 | 29860 | | $4.46 \times 10^{13}$ | | $1.2 \times 10$ |
| 1-butene → propenyl-1 + $CH_3$ | 25100 | 25100 | 25620 | | $1.02 \times 10^{16}$ | | $1.02 \times 10^4$ |
| 1-butene → $C_2H_3$ + $C_2H_5$ | 35000 | 35000 | 35540 | | $1.51 \times 10^{16}$ | | $5.81 \times 10^4$ |
| 1-butene → methycyclopropane | 3400 | 25494 | | | $6.92 \times 10^{14}$ | | $4.2 \times 10^{-1}$ |
| methycyclopropane → $C_4H_8$-1 | −3400 | 22094 | | 22559 | $2.34 \times 10^{15}$ | $1.1 \times 10^{15}$ | 2.4 |
| methycyclopropane → *cis*-2-$C_4H_8$ | −4000 | 21674 | | 22139 | | $4.0 \times 10^{14}$ | 2.4 |
| methycyclopropane → *trans*-2$C_4H_8$ | −4300 | 22234 | | 22699 | | $5.6 \times 10^{14}$ | 2.4 |
| methycyclopropane → *iso*-$C_4H_8$ | −4900 | 22759 | | 23224 | | $6.5 \times 10^{14}$ | 2.4 |
| *cis*-2-butene→ $C_4H_7$ + H | 30800 | 30800 | 31360 | | $1.34 \times 10^{14}$ | | $1.2 \times 10$ |
| *trans*-2-butene → $C_4H_7$ + H | 30800 | 30800 | 31360 | | $1.34 \times 10^{14}$ | | $1.2 \times 10$ |
| isobutene → $C_4H_7$ + H | 30800 | 30800 | 31360 | | $1.34 \times 10^{14}$ | | $1.2 \times 10$ |

[a] Taken from ref 19. [b] Calculated from either bond dissociation energy, $\Delta E$, or literature value of $E_a$ and transformed to $E_0$. [c] $E_0$ corrected for thermal energy of reactant and transition state. [d] Taken from ref 22. [e] Calculated at 298 K using geometry and frequencies from B3LYP calculations.

**TABLE 4: Calculated Structural and Energy Parameters for the $C_4H_8$ System**

| species | I $10^{-40}$ g $cm^2$ | $\langle E\rangle_{298}{}^a$ $cm^{-1}$ | frequencies $cm^{-1}$ |
|---|---|---|---|
| $C_4H_8$-1 | 28.4, 215, 234 | 550 | 124, 241, 289, 463, 526, 819, 827, 893, 986, 993, 1010, 1062, 1134, 1224, 1285, 1302, 1399, 1413, 1451, 1473, 1480, 1658, 2921, 2938, 2943, 2995, 3004, 3018, 3031, 3106 |
| methycyclopropane | 53.8, 133, 152 | 420 | 216, 326, 351, 744, 770, 793, 842, 914, 967, 1027, 1038, 1077, 1111, 1163, 1174, 1197, 1359, 1395, 1437, 1463, 1471, 1480, 2919, 2977, 2980, 3017, 3021, 3024, 3087, 3101 |
| $C_4H_8$-TS-c3h[b] | 39.6, 221, 230 | 700 | 174, 202, 266, 310, 391, 482, 577, 740, 864, 879, 970, 984, 999, 1112, 1221, 1271, 1314, 1374, 1431, 1446, 1466, 1565, 2866, 2981, 3034, 3039, 3053, 3080, 3139 |
| $C_4H_8$-TS-c3c4[c] | 77.0, 415, 456 | 1080 | 16, 73, 91, 222, 228, 409, 524, 550, 572, 762, 816, 909, 988, 1008, 1220, 1251, 1380, 1381, 1397, 1484, 1534, 3032, 3039, 3049, 3063, 3137, 3155, 3207, 3209 |
| $C_4H_8$-TS-c2c3[d] | 46.9, 559, 591 | 1050 | 17, 84, 101, 120, 204, 265, 619, 701, 764, 790, 879, 940, 1000, 1054, 1166, 1352, 1358, 1432, 1435, 1459, 1605, 2804, 2891, 2942, 2996, 3005, 3073, 3093, 3169 |
| methcyc-TS[e] | 104, 188, 264 | 920 | 87, 110, 119, 209, 315, 407, 444, 557, 893, 908, 921, 984, 1039, 1158, 1277, 1374, 1406, 1414, 1449, 1471, 1633, 2776, 2842, 2 922, 2981, 3009, 3032, 3038, 3115 |

[a] Average thermal energy at 298 K with zero of energy taken as the zero point energy of the species. [b] Transition state for reaction 10. [c] Transition state for reaction 9. [d] Transition state for reaction 8. [e] Transition state for reactions 4, 5, 6, 7, −4, −5, −6, and −7.

within each energy manifold so that collisional stabilization of $R_i$ requires a sequence of collisions. The end of a sequence occurs when the internal energy is less than the lowest critical energy for reaction of that species. The weak collider is described by a collision probability model, $P(E',E)$ in which the internal energy is $E$ before the collision and $E'$ after. For the present calculations an exponential model is used,

$$P(E',E) \propto \exp(-(E' - E)/\langle\Delta E\rangle_d) \text{ for } E' \leq E$$

with the average energy removed per "down" ($E' \leq E$) collision, $\langle\Delta E\rangle_d$ set at 400 $cm^{-1}$.

The Marcus−Rice formulation (RRKM)[16] was used to calculate the microcanonical unimolecular rate coefficients. The required vibrational frequencies of the "reactants" and transition states were calculated using Gaussian 98[17] with a 6-31 G(d) basis set using DFT with B3LYP functionals. Vibrational frequencies for stable reactants were calculated from fully optimized geometries, while those for transition states involving simple decomposition were calculated from optimized geometries with the breaking of C−C or C−H bonds set to 0.45 or 0.30 nm, respectively. For decyclization reactions, the critical energy was assigned to the maximum energy along the path when the appropriate C−C bond length was sequentially incremented and the other coordinates optimized. Vibrational frequencies calculated from the optimized geometry were scaled by a factor of 0.9613.[18] Because the spirit of this paper is to semiquantitatively assess the importance of various pathways, a more accurate but more computationally intensive variational transition state calculation was not used. The results of these simplified and computationally less demanding calculations are tabulated in Tables 3 and 4 .

The RRKM calculations also require critical energies for the reactions and structural quantities (moments of inertia and vibrational frequencies) for both reactants and transition states. The procedure we used in determining the appropriate values is described below.

For thermal systems, the rate coefficient for unimolecular reactions can be efficiently parametrized using macroscopic Arrhenius parameters: $A$ (pre-exponential factor) and $E_a$ (activation energy). These parameters can also be computed from electronic structure calculations using the generated critical energy, vibrational frequencies, and geometry. Although the present system involves a nonthermal distribution of 1-butene reactants, it is beneficial to compare calculated $A$ and $E_a$ factors for the reactions in this system with those previously reported for the same or similar reactions. The comparison is helpful in bracketing the derived $A$ and $E_a$ quantities into feasible sets. The approach is to use the calculated vibrational frequencies to model the energy dependence of the microscopic rate coefficients and the published activation or critical energies and $A$ factors from the literature or analogous reactions to simulate the observations.

*Critical Energies: Thermodynamics and Energetics.* Thermodynamic parameters for the stable and radical species were obtained from the NIST DATABASE accessed through the web[19] and are also listed in Table 3. Estimates based on bond dissociation energies and heats of formation were made for those

species where the values have not been reported. The bond energies determined from the B3LYP calculations were consistently **smaller** than the reported experimental values. The critical energies for reactions involving simple bond rupture, C−H or C−C, were set to the endoergicity of the specific reaction, i.e., it was assumed that there was no barrier for the reaction of a radical with another radical or H atom. However, the critical energies determined from the reaction path for the B3LYP calculations indicated a barrier **higher** than the endoergicity of the reaction.

*Structure, Vibrational Frequencies, and A Factors.* The calculated and reported *A* factors for the reactions involving C−C bond rupture are within a factor of 2 of each other.[20] They are large, $10^{16}-10^{17}$ $s^{-1}$, about $10^3-10^4$ larger than those for "normal" unimolecular reactions. This is predominately a result of the "loose" transition state for these reactions. When the transition state structure is indistinguishable from the products, this factor would just be the ratio of partition functions for the vibrational and rotational modes of products to reactants. As seen in Table 3, the $Q_{vr}$(products)/$Q_{vr}$(reactant) values are of the order of $10^5$. Thus, because $A < 10^{18}$ $s^{-1}$, it can be concluded that there are geometric constraints on these transitional modes in the transition state.

The *A* factors for C−H bond rupture are expected to be smaller than that for C−C bond rupture because the transitional modes for the departing H− atom become only translations, i.e., there are no rotations. This is shown by the $Q_{vr}$(products)/$Q_{vr}$(reactant) values in Table 3, which are of the order of 10, i.e., ∼1000 times smaller than when two polyatomic fragments are formed by the rupture. This is understood because each rotation contributes a factor of ∼10 to the partition function of the products so that three rotations for a nonlinear polyatomic fragment would generate a factor of $10^3$. From these values, it would be expected that the *A* factor for C−H rupture would be $10^{13}-10^{14}$ $s^{-1}$; the present calculations lead to a value of $4.46 \times 10^{13}$ for 1-butene and *cis*-2-butene and $1.34 \times 10^{14}$ $s^{-1}$ for *trans*-2-butene and isobutene, respectively. The difference between these two groups of reactants is primarily due to the different reaction path degeneracies. The discrepancies for the C−H bond rupture between calculated and reported/estimated *A* factors should be noted; for butane and 1-butene,[21] they are $1.58 \times 10^{16}$ and $1.26 \times 10^{15}$ $s^{-1}$, respectively. In this case, the values are between 10 and 100 times larger than those calculated here. Similarly, large *A* factors for the C−H bond rupture in 2-butyne and 1,3-butadiene have been estimated[22] to be $1.5 \times 10^{16}$ and $4.4 \times 10^{15}$ $s^{-1}$, respectively. The experimental values for C−H bond rupture are difficult to determine because competitive processes involving C−C bond rupture have larger rate coefficients (both a larger *A* factor and lower critical energy) and thus dominate the competition. Thus, in thermal systems, the C−H decomposition channel is not competitive and large errors in determining *A* and $E_a$ are to be expected. For a given rate coefficient an increase in $E_a$ by 4 kJ/mol generates a 5-fold increase in the *A* factor. In chemically activated systems, a similar correlation exists.

Modeling of the $CH_3 + C_2H_3$ experimental results generated values of $5 \times 10^{15}$ and $2.2 \times 10^{14}$ $s^{-1}$ for the allylic C−H and vinylic $CH_3$−C bond ruptures at 298 K in propene, respectively.[11] The smaller *A* value for C−C rupture may be due to a tighter transition state than for allylic or saturated C−C ruptures and is consistent with the 1,3-butadiene results. These results are interesting and indicate the need for more direct experiments in which both the equivalent of *A* and $E_a$ can be independently determined. Nonetheless, the exact *A* factor will depend upon the relative constraints of the transitional modes for these two reactions and any restricted motions in the radical fragment. We believe the reported values of $A > 10^{15}$ $s^{-1}$ for C−H bond ruptures are too large and that further work is needed in this area.

*Computational Predictions.* Calculations for the decomposition of butane (details not reported here) resulting from the combination of ethyl radicals indicate that, at the lowest pressures of the present experiments, all of the butane is collisionally stabilized. Therefore, there is no pressure dependence of the butane yield at pressures used in the current study. This is also consistent with the previously reported experiments.[12]

The 1-butene formed by the combination of ethyl and vinyl radicals has about 419 kJ $mol^{-1}$ (35 000 $cm^{-1}$) of internal energy and an average thermal energy of 6.6 kJ $mol^{-1}$ (550 $cm^{-1}$) for a total internal energy of ∼426 kJ $mol^{-1}$ (35 500 $cm^{-1}$). This is ∼53 kJ $mol^{-1}$ (4500 $cm^{-1}$) more internal energy than when ethyl radicals combine to give butane. Not only does the chemically activated 1-butene have more energy than chemically activated butane from the formation of two $C_2$ fragments, it also can react with lower critical energies via the rupture of allylic $C_3$−H and $C_3$−$C_4$ bonds and the cyclization to methyl cyclopropane. However, because C−C bonds are generally weaker than C−H bonds the paths involving vinylic $C_{1\ or\ 2}$−H bond and aliphatic $C_4$−H bond rupture require additional energy above the internal energy provided by the combination reaction. The path involving allylic $C_3$−H bond rupture has a critical energy of ∼75 kJ $mol^{-1}$ (6300 $cm^{-1}$) below the internal energy provided by the combination reaction. The allylic $C_3$−$C_4$ bond rupture channel has a critical energy that is ∼125 kJ $mol^{-1}$ (10 500 $cm^{-1}$) lower than the available internal energy. Isomerization (cyclization) of 1-butene to methylcyclopropane involves a H-atom migration with a new C−C bond being formed at the expense of the $\pi$-bond. The calculated 413 kJ $mol^{-1}$ (34 500 $cm^{-1}$) critical energy for the isomerization of methycyclopropane to 1-butene was found to be substantially larger than the reported activation energy of 270 kJ $mol^{-1}$ (22 570 $cm^{-1}$). Hence, the reported Arrhenius activation energies of the decyclization reactions (4, 5, 6, 7) for the thermal isomerization of methylcyclopropane were used.[24] The large difference between the calculated and the experimentally derived critical energies may be due to the complex nature of this particular transition state that involves C−C bond rupture, the formation of a C−C $\pi$ bond, and a H− atom migration. Although there is a large discrepancy between the calculated critical energy and observed energetics for this decyclization, the calculated *A* factor ($2.34 \times 10^{15}$ $s^{-1}$) is in good agreement with the reported value of $1.05 \times 10^{15}$ $s^{-1}$.[25] This value for *A* is within the expected range for a decyclization reaction in which the product has free internal rotations. The potential energy profile for these reactions is shown in Figure 2.

The relative magnitude of critical energies for reaction of 1-butene should be noted: isomerization (cyclization) ∼ allylic C−C bond rupture < allylic C−H bond rupture < C−C bond rupture. The zero of energies for the *cis*-, *trans*-, and *iso*-butene isomers are lower than that for 1-butene, which is also lower than that for methylcyclopropane. Thus the isobutene is the thermodynamically favored product.

The rate coefficients for the reactions depicted in Figure 2 are shown in Figure 3. Also shown is the nascent energy distribution function, $f(E)$, for the combination product as a function of temperature. Not including the reverse reaction forming 1-butene (reaction 8), these reactions can be classified

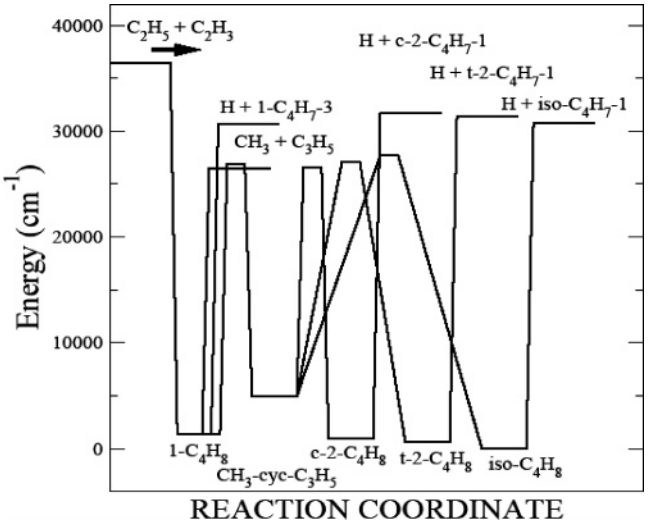


**Figure 2.** Potential energy profile for the ethyl + vinyl combination reaction; the lowest energy (isobutene) has been set to the zero of energy ($cm^{-1}$).

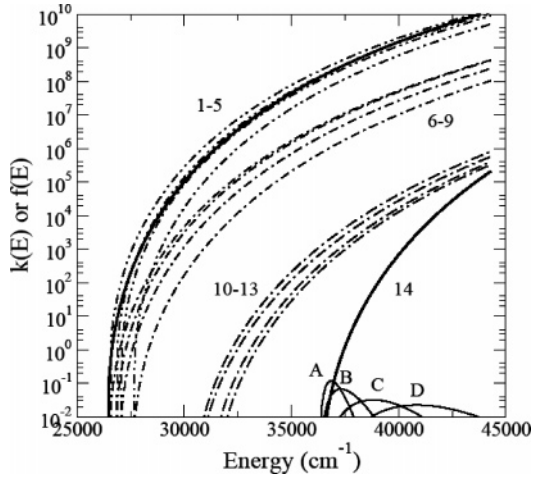


**Figure 3.** Plots of energy-dependent rate coefficients [$k(E)$, $s^{-1}$] for the reactions depicted in Figure 2 grouped as: decyclization of methylcyclopropane [short dash−dot−dot lines] (curves 1, 2, 4, and 5 corresponding to reactions 5, 4, 6, and 7, respectively), cyclization to methylcyclopropane [short dash−dot lines] (curves 6−9 corresponding to reactions −5, −4, −6, and −7, respectively), allylic C−H rupture [long dash−dot lines] (curves 10−13 corresponding to reactions 10, 13, 12, and 11, respectively), and C−C rupture [heavy solid lines] (curves 3 and 14 corresponding to reactions 9 and 8, respectively). Curves A−D [light solid line] represent the nascent energy distribution functions, $f(E)$, for the combination product (1-butene) at 200, 298, 500, and 700 K, respectively.

into four groups: (a) decyclization (reactions: 4, 5, 6, 7), (b) cyclization (reactions −4, −5, −6,-7), (c) allylic C−H rupture (reactions: 10, 11, 12, 13), and allylic C−C rupture (reaction: 9). The $k(E)$'s ($s^{-1}$) for the average energy at 298 K are: (a) $\sim 5 \times 10^8$, (b) $\sim 5 \times 10^6$, (c) $\sim 2 \times 10^4$, and (d) $\sim 5 \times 10^8$, respectively. At a pressure of 1 Torr, the pseudo first-order rate coefficient for bimolecular collisions is $\sim 10^7$ $s^{-1}$. Thus, at 1 Torr, only processes with $k(E) \geq 10^7$ $s^{-1}$ (decyclization and allylic C−C bond rupture) will be competitive with collisional stabilization. Consequently, for pressures above 10 Torr, the cyclization of 1-butene to methylcyclopropane can be ignored, so the coupled reactions of the five $C_4H_8$ isomers are decoupled and the chemically activated 1-butene is only depleted by the allylic C−C rupture, i.e., only $S_1$ and $D_1$ are important. Curve 2 in Figure 1 is a least-squares fit of the experimental data with a model in which the limiting high-pressure ratio and the

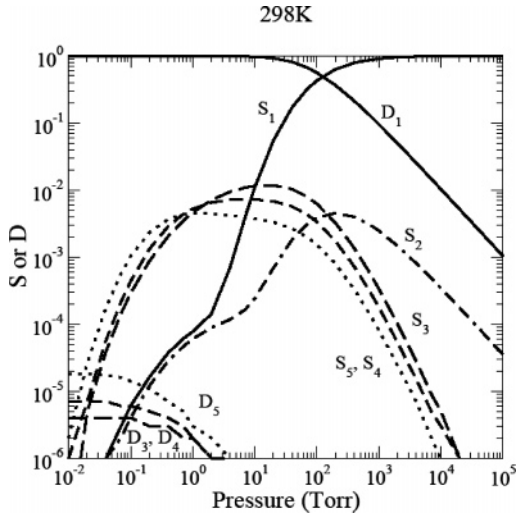


**Figure 4.** Plots of stabilization ($S$) and decomposition ($D$) of $C_4H_8$ products from the $C_2H_5 + C_2H_3$ combination reaction vs pressure at 298 K. The 1−5 subscripts correspond to 1-butene, methylcyclopropane, *cis*-2-butene, *trans*-2-butene, and isobutene, respectively. $D_1$ is the decomposition resulting from the allylic C−C rupture while $D_3$, $D_4$, and $D_5$ correspond to the allylic C−H rupture from *cis*-2-butene, *trans*-2-butene, and isobutene, respectively.

apparent rate coefficient for reaction 9 ($k_a$) is optimized with $k_a = \omega D_1/S_1$ where $D_1 + S_1 = 1.0$. The optimized high-pressure ratio is 1.3. The difference between the simplified model (curve 2) and master equation calculation (curve 1) at low pressure is due to the effect of weak collisions. The simplified model treats weak collisions as a strong collider with a constant inefficiency independent of pressure, while the master equation generates steady-state populations that are nonlinear with pressure, i.e., weak collider "turnup" is displayed. Because of the size of the experimental errors, a least-squares calculation using the master equation model was not made.

The calculated pressure dependence of the combination and subsequent "decomposition" products when all five isomers are included at 298 K is shown in Figure 4. At pressures less than 0.01 Torr, the slower C−H bond rupture is faster than collisional stabilization but still less than 0.00001 of the allylic C−C bond rupture. Below 1 Torr, the various $C_4H_8$ isomers are in a pseudo-equilibrium. Allylic $C_3-C_4$ rupture is ∼100% at 1 Torr and decreases to 50% at 100 Torr. At pressures above 1000 Torr, the 1-butene is effectively stabilized by collisions and there is no decomposition. Thus, at pressures less than 50 Torr, the dominant stable products will be products that result from the reactions of methyl and allyl radicals with other species present in the reaction cell. These curves indicate that the stabilization of nascent $C_4H_8$, $S_1$, and the total decomposition, $D_1$, will account for >99% of the chemically activated 1-butene that is formed. This is consistent with the experimental observations and the decoupling of the reaction scheme. Experimental methods used in this study cannot identify potential cis/trans isomeric forms of the products, thus a direct comparison with calculation is not possible.

For pressures up to 1 Torr, the yields of stabilized *cis*-2-butene, *trans*-2-butene, and isobutene isomers exceed the yields of stabilized 1-butene and methylcyclopropane isomers. At 1 Torr, the yields of stabilized 1-butene and methylcyclopropane continue to increase with increasing pressure, while the *cis*-2-butene, *trans*-2-butene, and isobutene yields reach a plateau and then decrease due to their sequential formation pathway. For pressures above 100 Torr, the yield of methylcyclopropane plateaus and begins to decrease with increasing pressure. At

1000 Torr, collisional stabilization dominates and only 1-butene should be observed as is experimentally confirmed. Between 10 and 100 Torr methylcyclopropane is ~1% of the 1-butene; above 100 Torr, the methylcyclopropane yield rapidly decreases. The isobutene and 2-butene isomers have yields greater than 1-butene for pressures less than ~10 Torr; above 10 Torr, the amounts of these isomers become progressively smaller relative to 1-butene.

*Pressure Effect: $k_c$ and 1-$C_4H_8$ Yield.* As illustrated in Figure 4, the amount of stabilized 1-$C_4H_8$, $S_1$, formed by the combination of $C_2H_5$ and $C_2H_3$, increases with increasing pressure and is within 90% of the high-pressure limit at ~1000 Torr. Thus, for pressures below the high-pressure limit, the yield of 1-$C_4H_8$ depends on: $S_1$, $k_{1c}$ and the concentration of ethyl and vinyl radicals. The $C_4H_{10}$ produced from the combination of $C_2H_5$ and $C_2H_5$ is completely collisionally stabilized at the pressures of the present experiment so that the $C_4H_{10}$ yield is a measure of only $k_{2c}$ and the ethyl radical concentrations. The ratio of the yields, $[1\text{-}C_4H_8]/[C_4H_{10}] = R_{12c}$, exhibits a pressure dependence due to the pressure dependence for the stabilization of 1-$C_4H_8$.

$$R_{12c}(\mathrm{p}) = k_{1c} \times \int [C_2H_5(t)]\,[C_2H_3(t)]\,dt \times S_1/k_{2c} \times \int [C_2H_5(t)]\,[C_2H_5(t)]\,dt$$

In the high-pressure limit, $S_1 = 1$ so that $R_{c12}(\infty)$ is given by

$$R_{12c}(\infty) = (k_{1c}/k_{2c}) \times \left(\int [C_2H_5(t)]\,[C_2H_3(t)]\,dt \Big/ \int [C_2H_5(t)]\,[C_2H_5(t)]\,dt\right)$$

Computer simulations for the present system indicated that the ethyl and vinyl radicals, resulting from the 193 nm photolysis of EVK, are nearly equal[8] and that the ratio of integrals is pressure independent so that

$$R_{12c}(\mathrm{p})/R_{12c}(\infty) = S_1$$

and

$$R_{12c}(\mathrm{p}) = S_1 \times R_{12c}(\infty)$$

The experimental results shown in Figure 1 and the high-pressure limit from Figure 4 suggest that $R_{12c}(\infty) \sim 1.3$. Unfortunately, the present apparatus cannot operate at pressures in excess of 1 atm, so this cannot be tested.

Plots of $R_{12c}$ (p) vs pressure for various input variables are also shown in Figure 1 with $R_{12c}(\infty) = 1.3$. Although the reaction scheme appears complex for pressures >1 Torr, the pressure dependence of $S_1$ depends on the competition between collisional stabilization and the allylic C−C bond rupture in 1-butene (reaction 9). Curve 1 is the master equation model calculation using the vibrational frequencies from the B3LYP calculations and is a reasonable fit to the data. For this model, the Arrhenius prexponential factor, $A$, is $1.02 \times 10^{16}$ s$^{-1}$ and $E_o = 25\,100$ cm$^{-1}$. The sensitivity of these plots to $A$ and $E_0$ are seen in curves 3 and 4. An increase in $E_0$ to 26 100 cm$^{-1}$ shifts curve 1 to lower pressures (curve 3a), while decreasing $A$ (multiplying by 0.3) also shifts curve 1 to lower pressure (curve 4a). Likewise, decreasing $E_0$ to 24 100 cm$^{-1}$ shifts curve 1 to high pressure (curve 3b), or increasing $A$ by a factor of 3 results in a shift to higher pressure (curve 4b). With these parameters, the experiments can be bracketed with: $3 \times 10^{15} < A < 3 \times 10^{16}$ s$^{-1}$ and $24\,100 < E_0 < 26\,100$ cm$^{-1}$. These "nonfitted" results are in good agreement with the recently reported[25] measurements for the allylic C−C bond rupture in 1-butene formed by the combination of methyl + allyl radicals: $A = 1.1 \times 10^{16}$ s$^{-1}$ and $E_0 = 26500$ cm$^{-1}$ ($E_a$ was reported as 39 100/$R$ = 27 200 cm$^{-1}$).

From our experiments, only the magnitude of the energy dependent rate coefficient can be determined, i.e., there is not a unique set of vibrational frequencies and $E_0$ that will fit the data. In thermal activation systems, the temperature dependence of the rate coefficient allows both $A$ and $E_a$ to be calculated; similar experiments could be performed for a chemical activation system. The correlation between $A$ and $E_0$ can be determined by using an equivalent Arrhenius relation: $k = A \exp(-E_0/c)$, where $c$ is a measure of the excitation energy or an RRK expression: $k = A(E/E_0 - 1)^{n-1}$, where $n$ is the "effective" number of oscillators. Both $c$ and $n$ can be calculated from the $k(E)$'s for reaction 9 in Figure 3. For the present calculations, both of these models correlate a 1000 cm$^{-1}$ difference in $E_0$ with a factor of 3 in the Arrhenius $A$ factor.

*Comparison of Pressure Effects: $C_2H_5 + C_2H_3$ and $CH_3 + C_2H_3$.* The present calculations for the 1-butene system can be compared to the results reported independently by Fahr et al.,[5] Thorn et al.,[9] and Stoliarov et al.[10] for the $CH_3 + C_2H_3$ reaction at 298−300 K. In that as well as $C_2H_5 + C_2H_3$, the combination products can isomerize to a cyclopropane or rupture allylic $C_3$−H bonds; additionally, the $C_4H_8$ system also includes the $C_3$−$C_4$ allylic bond rupture, which has a lower critical energy and larger $A$ factor than that for the C−H bond rupture in the $C_3H_6$ system. For the same excess energy ($E - E_0$), the $C_3H_6$ system has larger $k(E)$'s [$8 \times 10^6$ vs $3 \times 10^3$ s$^{-1}$] (a factor of ~3000 larger) due to the smaller density of states for $C_3H_6$ compared to $C_4H_8$. This would be even greater if the excitation energies were the same.

For a unimolecular system in thermal equilibrium, the observed rate coefficients would not have this dependence on the density of states and the $k(T)$ would be identical if the critical energies were equal. If this were the only factor, the high-pressure limit for the $C_3H_6$ system would occur at a higher pressure than that for the 1-$C_4H_8$ system. However, the high-pressure limit for the 1-$C_4H_8$ system occurs at a higher pressure than the $C_3H_6$ system due to the dominance of the allylic C−C bond rupture; the $k(E)$'s for the allylic C−C bond rupture are $\sim 2 \times 10^5$ times larger than that for the allylic C−H bond rupture. Thus the half pressure, $p_{0.5}$, at which $S = 0.5$ occurs is 100 Torr for the 1-$C_4H_8$ system and 2 Torr for the $C_3H_6$ system; the plots of $S$ vs pressure are shown in Figure 5 along with the experimental points. This difference in $p_{0.5}$ produces ~20% decomposition in the $C_3H_6$ system and ~90% decomposition in the $C_4H_8$ system at 10 Torr; at 100 Torr, the decompositions reduce to ~2% and 60%, respectively. If only the allylic C−H bond rupture was open in the 1-$C_4H_8$ system, that curve would have a $p_{0.5}$ multiplied by a factor of $\sim 5 \times 10^{-6}$!

*Temperature Dependence of $C_2H_5 + C_2H_3$.* It is informative to observe how the product distribution changes with temperature and how this affects the apparent combination rate coefficient. Calculations at 200 and 700 K are shown in Figures 6 and 7. As the temperature increases from 200 to 700 K, the average thermal energy for the chemically activated 1-$C_4H_8$ increases from 630 to 5050 cm$^{-1}$; this is on top of the 35 000 cm$^{-1}$ produced exoergicity of the combination reaction. These plots show that the amount of C−H bond rupture increases with increasing temperature and that an increase in temperature increases the pressure for complete stabilization. This is a result of both increasing the average energy of the

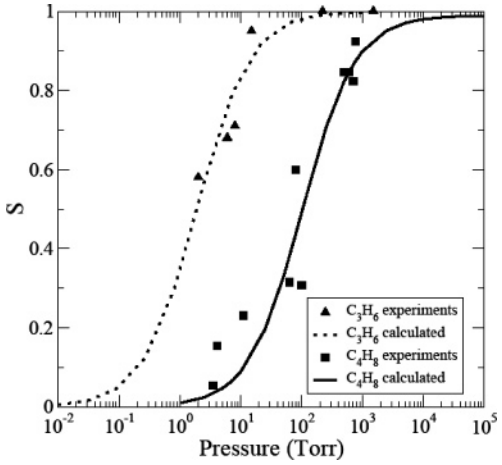


**Figure 5.** Plots of stabilization (*S*) vs pressure for the (a) $CH_3 + C_2H_3$ combination reaction: calculated (dotted line) and experimental points (filled triangles) and (b) $C_2H_5 + C_2H_3$ combination reaction: calculated (solid line) and experimental points (filled squares) at 298 K. Experimental points taken from ref 5 for the $CH_3 + C_2H_3$ system.

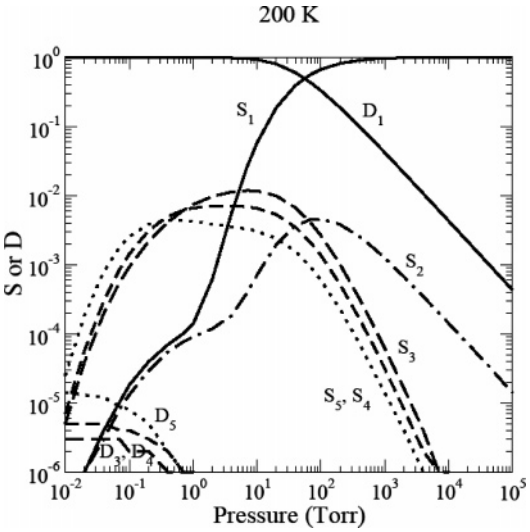


**Figure 6.** Plots of stabilization (*S*) and decomposition (*D*) of $C_4H_8$ products from the $C_2H_5 + C_2H_3$ combination reaction vs pressure at 200 K. See Figure 4 caption for detailed legend.

chemically activated product and the increased importance of "up" collisions with increasing temperature.

Further, the temperature dependence for $S_1$ vs pressure is shown in Figure 8. With increasing temperature the curves shift to higher pressure, i.e., a higher pressure is required for stabilization. Note that the pressure where $S_1 = 0.5$ increases from 40 Torr at 200 K to 3000 Torr at 700 K. Clearly, decomposition becomes increasingly important at high temperatures, and $C_4H_8$ is only quenched at correspondingly high pressures.

## Conclusions

The pressure dependence of the product channels for the cross-combination of $C_2H_5$ and $C_2H_3$ radicals was measured from 4 to 760 Torr (about 0.5 to 101 kPa); products (butane and 1,3 butadiene) resulting from the self-combination were also observed and monitored. At high pressure, the relative yields of 1-butene and butane provide information on the rate coefficients for the associated combination reactions. The pressure dependence of these yields is a function only of the cross combination reaction because the chemically activated

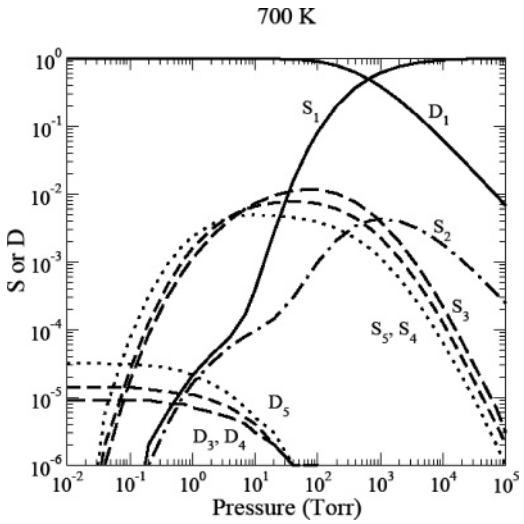


**Figure 7.** Plots of stabilization (*S*) and decomposition (*D*) of $C_4H_8$ products from the $C_2H_5 + C_2H_3$ combination reaction vs pressure at 700 K. See Figure 4 caption for detailed legend.

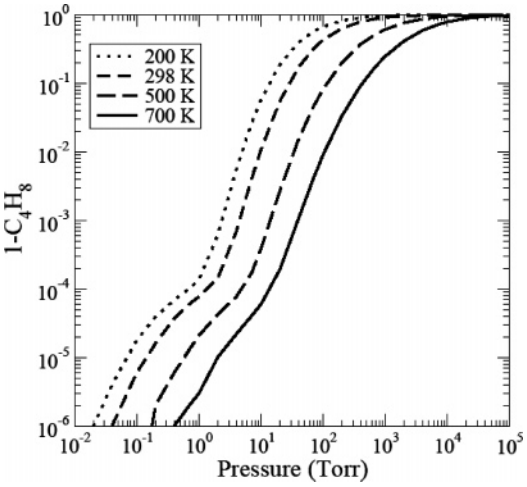


**Figure 8.** Calculated curves for [1-$C_4H_8$], i.e., $S_1$, vs pressure at temperatures of 200 K (dotted line), 298 K (short dashed line), 500 K (long dashed line), and 700 K (solid line).

butane formed by the self-combination does not have sufficient energy to break stronger C−H or C−C bonds. On the other hand, chemically activated 1-butene is formed with a higher internal energy than butane and has "weaker" C−H and C−C bonds that can rupture. Thermodynamics point to a series of cyclization/decyclization isomerizations and C−C and C−H bond ruptures that involve five $C_4H_8$ isomers: 1-butene, methylcyclopropane, *cis*-2-butene, *trans*-2-butene, and isobutene. The products resulting from low-pressure experiments suggest a very complex mechanistic behavior. The $[C_4H_8]/[C_4H_{10}]$ ratio decreased with pressure due to decomposition of the chemically activated 1-$C_4H_8$ in which the weak allylic C−C bond is broken leading to the reaction: $H_2C{=}CHCH_2CH_3 * \rightarrow C_3H_5 + CH_3$. Such processes occur even at moderate pressures (~200 Torr) and become more significant at lower pressures. Products of the mixed allyl, methyl, ethyl, and vinyl radicals combination reactions have been observed.

The radical−radical reactions involving ethyl and vinyl radicals reported in this paper and our previous work allow for a systematic evaluation of energetic and structural parameters that are important in the understanding of hydrocarbon reactions. Four classes of reactions are important in this system: allylic C−C bond rupture, allylic C−H bond rupture, and cyclization/

decyclizations involving H atom migration. While a comprehensive experimental characterization is not possible, even a small number of measurements can provide support for a calculational description of the reaction system.

The presence of $\pi$ bonds in the reactants and products affect both the excitation energy and the critical energy for competitive reaction paths available to the nascent combination products; C−C and C−H rupture from allylic positions are particularly accelerated. At very low pressures where there is a pseudoequilibrium between the $C_4H_8$ isomers, the allylic C−C bond rupture from 1-butene dominates; less than $10^{-5}$ of the total decomposition is via allylic C−H bond rupture. With increasing pressure, the yield of 1-butene increases at the expense of the other isomers. Around 100 Torr, stabilization becomes equal to decomposition. Although the 1-butene yield at low pressures is complex due to the reversible production of other $C_4H_8$ isomers, the yield of stabilized 1-butene follows a "simple" pressure dependence above 10 Torr at 298 K. Increasing temperature increases the average energy of the 1-butene and thus requires a higher pressure for stabilization.

The pressure dependence of the combination/disproportionation ratio for the cross reaction is determined solely by the combination reaction because the two fragments resulting from disproportionation has insufficient energy to promote unimolecular processes. The limiting high-pressure ratio for $[C_4H_8]/[C_4H_{10}]$ of 1.3 indicates that the rate coefficient for the combination of vinyl and ethyl radicals is 1.3 times larger for the combination of ethyl radicals.

**Acknowledgment.** Fahr and Halpern wish to acknowledge partial support of this work by NASA-Planetary Atmospheres Research Program (award no. NNG05GQ15G).

**Supporting Information Available:** Examples of GC/MS/FID traces for two different pressure conditions. This material is available free of charge via the Internet at http://pubs.acs.org.

## References and Notes

(1) Miller, J. A.; Melius, C. F. *Combust. Flame* **1992**, *91*, 21 and references therein.

(2) Gardner, W. C., Jr. *Combustion Chemistry*; Springer-Verlag: New York, 1984.

(3) Westmoreland, P. R.; Dean, A. M.; Howard, J. B.; Longwell, J. P. *J. Phys Chem.* **1989**, *93*, 8171.

(4) Finlayson-Pitts, B. J.; Pitts, J. N., Jr. *Atmospheric Chemistry*; Wiley-Interscience: New York, 1986, and references therein.

(5) Fahr, A.; Laufer, A. H.; Tardy, D. C. *J. Phys. Chem.* **1999**, *103*, 8433.

(6) (a) Fahr, A.; Laufer, A. H. *J. Phys. Chem.* **1988**, *92*, 7229. (b) Fahr, A.; Laufer, A. H., *J. Phys. Chem.* **1990**, *94*, 726. (c) Fahr, A.; Laufer, A. H.; Klein, R.; Braun, W. *J. Phys. Chem.* **1991**, *95*, 3218.

(7) Thorn, R. P.; Payne, W. A.; Stief, L. J.; Tardy, D. C. *J. Phys. Chem.* **1996**, *100*, 13594.

(8) Fahr, A.; Tardy, D. C. *J. Phys Chem A* **2002**, *106*, 11135.

(9) Thorn, R. P.; Payne, W. A.; Chillier, X. D. F.; Stief, L. J.; Nesbitt, F. L. Tardy, D. C. *Int. J. Chem. Kinet.* **2000**, *32*, 304−316.

(10) Stoliarov, S. I.; Knyazev, V. D.; Slagle, I. R. *J. Phys. Chem. A* **2000**, *104*, 9687.

(11) Stoliarov, S. I.; Knyazev, V. D.; Slagle, I. R. *J. Phys. Chem. A* **2002**, *106*, 6952.

(12) Baulch, D. L.; Cobos, C. J.; Cox, R. A.; Frank, P.; Hayman, G.; Just, T.; Murrells, T.; Pilling, M. J.; Troe, J.; Walker R. W.; Waratz, J. *J. Phys. Chem. Ref. Data* **1994**, *23*, 847 and references therein.

(13) Fahr, A.; Laufer, A. H.; Klein, R.; Braun, W. *J. Phys. Chem.* **1991**, *95*, 3218.

(14) Fahr, A.; Braun, W.; Laufer, A. H. *J. Phys. Chem.* **1993**, *97*, 1502.

(15) Tardy, D. C. *J. Phys. Chem.* **1979**, *83*, 1021.

(16) (a) Marcus, R. A.; Rice, O. K. *J. Phys. Colloid Chem.* **1951**, *55*, 894. (b) Marcus, R. A. *J. Chem. Phys.* **1952**, *20*, 359.

(17) Frisch, M. J.; Trucks, G. W.; Schlegel, H. B.; Scuseria, G. E.; Robb, M. A.; Cheeseman, J. R.; Zakrzewski, V. G.; Montgomery, J. A., Jr.; Stratmann, R. E.; Burant, J. C.; Dapprich, S.; Millam, J. M.; Daniels, A. D.; Kudin, K. N.; Strain, M. C.; Farkas, O.; Tomasi, J.; Barone, V.; Cossi, M.; Cammi, R.; Mennucci, B.; Pomelli, C.; Adamo, C.; Clifford, S.; Ochterski, J.; Petersson, G. A.; Ayala, P. Y.; Cui, Q.; Morokuma, K.; Malick, D. K.; Rabuck, A. D.; Raghavachari, K.; Foresman, J. B.; Cioslowski, J.; Ortiz, J. V.; Stefanov, B. B.; Liu, G.; Liashenko, A.; Piskorz, P.; Komaromi, I.; Gomperts, R.; Martin, R. L.; Fox, D. J.; Keith, T.; Al-Laham, M. A.; Peng, C. Y.; Nanayakkara, A.; Gonzalez, C.; Challacombe, M.; Gill, P. M. W.; Johnson, B. G.; Chen, W.; Wong, M. W.; Andres, J. L.; Head-Gordon, M.; Replogle, E. S.; Pople, J. A. *Gaussian 98*; Gaussian, Inc.: Pittsburgh, PA, 1998.

(18) Frisch, A.; Frisch, M. J. *Gaussian 98 User's Reference*; Gaussian, Inc.: Pittsburgh, PA, 1999.

(19) NIST Chemistry Webbook; http:/webbook.nist.gov/chemistry.

(20) Benson, S. W. Thermochemical Kinetics; 2nd ed.; Wiley & Sons: New York, 1976.

(21) Dean, A. M. *J. Phys. Chem.* **1985**, *89*, 4600.

(22) Tsang, W.; Mokrushin, V. *Comubst. Inst. Proc.* **2000**, *28*, 1717.

(23) Tsang, W.; Mokrushin, V. *Mechanism and Rate Constants for 1,3 Butadiene Decomposition*, preprint; National Institute of Standards and Technology, Gaithersburg, MD, 2000.

(24) Kalra, B. L.; Cho, J. Y.; Lewis, D. K. *J. Phys. Chem. A* **1999**, *103*, 362.

(25) Knyazev, V. D.; Slagle, I. R. *J. Phys. Chem. A* **2001**, *105*, 3196.